Optical-pulse dynamics under quasi-$\mathcal{PT}$-symmetry

D. M. Tsvetkov, V. A. Bushuev, and B. I. Mantsyzov
Department of Physics, M. V. Lomonosov Moscow State University, Leninskie Gory, 119991 Moscow, Russia

(Received 17 December 2018; published 25 February 2019)

The parity-time ($\mathcal{PT}$)-symmetric optical properties are significantly restored for broadband radiation if the width of the field spectrum is substantially less than the width of the spectral line of a resonant medium. This is the so-called quasi-$\mathcal{PT}$-symmetry for broadband radiation. Under the quasi-$\mathcal{PT}$-symmetric light-matter interaction, we describe the dynamics of a short spatially localized pulse propagating in the extended medium, when the length of propagation significantly exceeds the pulse size. As an example, the boundary problem of dynamical Bragg diffraction in the Laue geometry for a short laser pulse in a photonic crystal (PhC) with strong material dispersion is solved. It is shown that at exceptional point of the $\mathcal{PT}$-symmetry breaking, the dynamics and parameters of the pulse change dramatically when the sign of the Bragg angle of incidence θ_B changes. Unidirectional zero Bragg reflection and unidirectional Bragg-diffraction-induced pulse splitting are revealed. At a positive angle, $\theta_B > 0$, the localized short pulse propagates in a quasi-$\mathcal{PT}$-symmetric PhC with gain and loss under Bragg diffraction condition as in a conservative transparent homogeneous medium. A change in the sign $\theta_B < 0$ leads to the appearance of an amplified diffracted pulse. In the case of a small detuning from the exact Bragg condition, at $\theta_B < 0$, the directions and magnitudes of the group velocities of different field modes change and, as a result, the temporal and spatial diffraction-induced pulse splitting occurs. Such asymmetric dynamics of the pulse propagation in a quasi-$\mathcal{PT}$-symmetric PhC can be used to effectively control the parameters and dynamics of short optical pulses by small changes in its frequency, in the magnitude of the gain and loss parameter of the medium, etc.

DOI: 10.1103/PhysRevA.99.023846

I. INTRODUCTION

A new direction of modern optics associated with the study of the optical properties of $\mathcal{PT}$-symmetric media, or non-Hermitian optics, has been actively developing over the last two decades [1,2]. Initially, physical systems invariant with respect to the parity-time transformation, or $\mathcal{PT}$-symmetric systems, were considered in problems of quantum mechanics, where it was shown that in the case of non-Hermitian systems with a $\mathcal{PT}$-symmetric complex potential, there can exist quantum states with real energy [3–5]. In $\mathcal{PT}$-symmetric optical systems with complex alternating dielectric permittivity $\varepsilon(x) = \varepsilon^*(-x)$, i.e., with gain and loss, new $\mathcal{PT}$-symmetric optical phenomena were discovered theoretically and experimentally. As examples we mention the propagation of $\mathcal{PT}$-symmetric modes and their breaking at an exceptional point [6–9], increased transparency under loss enhancement in dissipative structures [10], lasing and antilasing effects [11,12], unidirectional zero Bragg reflection in the Bragg [13–15] and the Laue geometries [16–21], etc. However, the Kramers-Kronig relation, which relates the real and imaginary parts of the dielectric permittivity of a resonant medium and follows from the fundamental principle of causality, permits the $\mathcal{PT}$-symmetry condition to be realized for a discrete set of frequencies only [22,23]. Therefore, linear optical $\mathcal{PT}$-symmetric phenomena have been studied mainly for monochromatic waves and beams. Recently [24], a method for significant restoring of the $\mathcal{PT}$-symmetric properties of dispersive media for broadband radiation with a finite continuous spectrum was proposed. The restoring is possible in the case of quasi-$\mathcal{PT}$-symmetry, when in a $\mathcal{PT}$-symmetric medium, the width of the inhomogeneous broadening spectral line of resonant impurities is much larger than the width of the propagating radiation spectrum. Thus, quasi-$\mathcal{PT}$-symmetry allows us to include the problems of the propagation dynamics of short localized optical pulses and nonmonochromatic beams in the number of problems of non-Hermitian optics.

In this paper, we demonstrate the dynamics of a *short spatially localized optical pulse* propagating in a quasi-$\mathcal{PT}$-symmetric medium with material dispersion. As an example, we study theoretically the propagation of a pulse in a quasi-$\mathcal{PT}$-symmetric photonic crystal (PhC) under dynamical Bragg diffraction in the Laue scheme "on transmission." Using the spectral method, the boundary problem of dynamical Bragg pulse diffraction in the two-wave approximation beyond paraxial approximation is solved. It is shown that although light-matter interaction in such medium is not exactly $\mathcal{PT}$-symmetric, the optical properties of the structure are close to $\mathcal{PT}$-symmetric ones, even at large propagation lengths of the order of tens of pulse sizes. We have described several quasi-$\mathcal{PT}$-symmetric optical phenomena for short broadband pulses. In particular, it is shown that near an exceptional point of the $\mathcal{PT}$-symmetry breaking at the central pulse frequency, a pulse with a finite continuous spectrum demonstrates not only a unidirectional zero diffraction reflection depending on the sign of the angle of radiation incidence on the structure, but also a change in the dynamics of pulse propagation and their mode structure—unidirectional Bragg-diffraction-induced pulse splitting. At a positive angle of incidence and a small deviation from the Bragg condition,

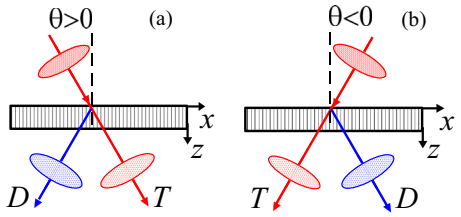

FIG. 1. Schematic representation of two cases of pulse incidence onto the PhC: (a) $\theta > 0$ and (b) $\theta < 0$; T and D are the transmitted and diffracted pulses, respectively.

the pulse propagates in a gain and loss medium as in a transparent and homogeneous one. A change in the sign of the incidence angle leads to a space-time splitting of the pulse, and, in addition, one of the pulses is formed by the amplified diffracted wave only and the other one by the transmitted and diffracted waves. Unlike the conservative PhC, the diffraction pulse splitting does not occur in the exceptional point under exact Bragg condition. Analytical estimations of the wave's amplitudes of different modes and their group velocities are in good agreement with the numerical results that take into account the finite pulse spectrum and the material dispersion of a resonant medium.

The paper is organized as follows. In Sec. II, we estimate the parameters for quasi-$\mathcal{PT}$-symmetric light-matter interaction. The boundary problem of the dynamical Bragg diffraction in the Laue scheme for a short laser pulse in quasi-$\mathcal{PT}$-symmetric PhC with dispersion is solved in Sec. III. In Sec. IV, we describe different regimes of dynamics of short localized pulse propagation in quasi-$\mathcal{PT}$-symmetric PhC. The results are summarized in Sec. V.

II. QUASI-$\mathcal{PT}$-SYMMETRY FOR BROADBAND RADIATION

Here we estimate analytically the decreasing of the parameter of deviation from $\mathcal{PT}$ symmetry in the case of quasi-$\mathcal{PT}$-symmetric light-matter interaction for broadband radiation and a rectangular inhomogeneous spectrum line of a resonant structure.

Let a short optical pulse with a central resonant frequency ω_0 and a finite spectral width $\delta\omega = 2/\tau$, where τ is the pulse duration, be incident onto a one-dimensional dispersive $\mathcal{PT}$-symmetric PhC (Fig. 1) with a dielectric permittivity

$$\varepsilon(x,\omega) = \varepsilon_0 + \varepsilon' \cos(hx) + i\hat{\varepsilon}(\omega)\sin(hx), \tag{1}$$

where $h = 2\pi/d$ is the modulus of reciprocal lattice vector $\mathbf{h}$, which is directed along the x axis, and d is the lattice period.

The first two terms $\varepsilon_0 + \varepsilon' \cos(hx) > 1$ in expression (1) describe a periodically modulated even function of the dielectric permittivity, which is determined by a transparent dielectric matrix with negligible material dispersion. The odd function $i\hat{\varepsilon}(\omega)\sin(hx)$ in Eq. (1) corresponds to the contribution to the dielectric permittivity of resonant two-level oscillators,

$$\varepsilon_{\rm res}(x,\omega) = i\hat{\varepsilon}(\omega)\sin(hx). \tag{2}$$

Here the spatially periodic function of the inversion of oscillators is chosen to be $w(x) = -\sin(hx)$. The dielectric permittivity of a dispersive resonant medium with two-level oscillators for a sufficiently long pulse with a duration $\tau \gg T_2$ is described by the complex function [24,25]

$$\hat{\varepsilon}(\omega) = i\beta \int_{-\infty}^{\infty} \frac{g(\Delta-\Delta_0)}{\Delta + i/T_2} d\Delta = \hat{\varepsilon}_R(\omega) + i\hat{\varepsilon}_I(\omega), \tag{3}$$

where

$$\hat{\varepsilon}_R(\omega) = \frac{\beta}{T_2}\int_{-\infty}^{\infty} \frac{g(\Delta-\Delta_0)}{\Delta^2 + 1/T_2^2} d\Delta,$$
$$\hat{\varepsilon}_I(\omega) = \beta \int_{-\infty}^{\infty} \frac{g(\Delta-\Delta_0)\Delta}{\Delta^2 + 1/T_2^2} d\Delta. \tag{4}$$

Here, $\beta = 4\pi N\mu^2/\hbar$, N is the concentration of resonant atoms, μ is the magnitude of the dipole moment of the transition of an atom, $\Delta = \omega - \omega_0'$ is the deviation of the radiation frequency ω from the resonance frequency of the atom ω_0', $\Delta_0 = \omega - \omega_0$ is the detuning of the field frequency from the central frequency of the resonance ω_0, T_2 is the time of transverse homogeneous relaxation of the dipole moment, and $g(\Delta - \Delta_0) = g(\omega_0 - \omega_0')$ is the function of inhomogeneous broadening of the spectral line.

Let us introduce the parameter of deviation from the exact $\mathcal{PT}$-symmetry condition: $\Delta_{PT}(x,\omega) = \varepsilon(x,\omega) - \varepsilon^*(-x,\omega)$ [26]; then it follows from Eqs. (1)–(3) that

$$\Delta_{PT}(x,\omega) = 2{\rm Re}\varepsilon_{\rm res}(x,\omega) = 2\hat{\varepsilon}_I(\omega)w(x). \tag{5}$$

From Eqs. (2) and (3), it can be seen that the quantity $\hat{\varepsilon}_I(\omega)$ determines the anti-$\mathcal{PT}$-symmetric odd contribution of resonant atoms, $-\hat{\varepsilon}_I(\omega)\sin(hx)$, to the real part of the dielectric permittivity (1). Thus, the material dispersion, $\hat{\varepsilon}_I(\omega) \neq 0$, violates the $\mathcal{PT}$ symmetry for an arbitrary value of the radiation frequency ω. However, the value $\Delta_{PT}(x,\omega)$ (5) can be significantly reduced and, therefore, the system $\mathcal{PT}$ symmetry in the region of the finite spectral width of a short pulse can be largely restored under increase of inhomogeneous line broadening [24], i.e., when quasi-$\mathcal{PT}$-symmetry for broadband radiation is implemented. Mathematically, this follows from the oddness of the integrand in expression $\hat{\varepsilon}_I(\omega)$ (4) in the case of an even function $g(\Delta - \Delta_0)$. Indeed, this is clearly seen in the example of a rectangular function of inhomogeneous broadening of the spectral line,

$$g(\Delta-\Delta_0) = \begin{cases} (\gamma_2^*\omega_0)^{-1}, & |\Delta-\Delta_0| \leqslant \gamma_2^*\omega_0/2, \\ 0, & |\Delta-\Delta_0| > \gamma_2^*\omega_0/2, \end{cases} \tag{6}$$

with width $\gamma_2^*\omega_0$, where $\gamma_2^* = 2/T_2^*\omega_0$ is the dimensionless inhomogeneous width of the spectral line, T_2^* is the time of inhomogeneous transverse relaxation of the dipole moment. From Eqs. (4)–(6), it follows that the parameter Δ_{PT} of the deviation from $\mathcal{PT}$ symmetry is proportional to $\hat{\varepsilon}_I(\omega) = \beta\Delta_0/(\gamma_2^*\omega_0)^2$. This quantity decreases rapidly with growth of the value γ_2^* if the width of the pulse spectrum $\delta\omega$ is substantially less than the width of the spectrum line of the resonant atom: $\delta\omega \sim \Delta_0 \ll \gamma_2^*\omega_0$. It is important to note that the antisymmetric part of resonant dielectric permittivity decreases much faster than the $\mathcal{PT}$-symmetric one: $|{\rm Re}\varepsilon_{\rm res}(x,\omega)/{\rm Im}\varepsilon_{\rm res}(x,\omega)| = 2|\Delta_0|/\pi\gamma_2^*\omega_0 \ll 1$. Therefore, the quasi-$\mathcal{PT}$-symmetry allows $\mathcal{PT}$-symmetric optical properties of the medium to be restored within the pulse spectrum under increase of inhomogeneous broadening γ_2^*.

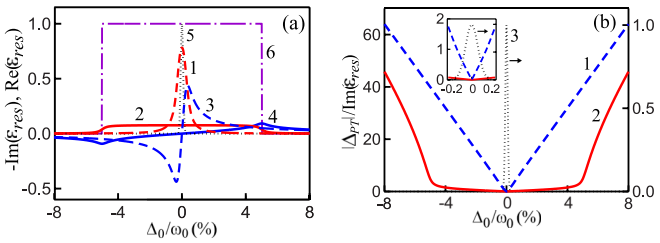

FIG. 2. (a) $-\mathrm{Im}(\varepsilon_{\mathrm{res}})$ (red lines 1 and 2) and $\mathrm{Re}(\varepsilon_{\mathrm{res}})$ (blue lines 3 and 4) vs frequency detuning at small $\gamma_2^* = 0.005$ (dashed lines 1 and 3) and large values of inhomogeneous broadening $\gamma_2^* = 0.1$ (solid lines 2 and 4) plotted for the points where $w(x) = 1$ compared with the spectrum $A_{in}(\Delta_0)$ of the pulse with duration $\tau = 1$ ps (dotted line 5) and with the inhomogeneous broadening function $g(\Delta_0)$ (line 6). (b) Dependence of $|\Delta_{PT}|/\mathrm{Im}(\varepsilon_{\mathrm{res}})$ on frequency detuning corresponding to (a) for $\gamma_2^* = 0.005$ (blue dashed line 1) and $\gamma_2^* = 0.1$ (red solid line 2) compared with the pulse spectrum (dotted line 3, right scale). Parameters: $\beta = 1/T_2$, $\gamma_2 = 0.005$, $\lambda_0 = 1$ μm. Inset: curves 1, 2, and 3 in a small area near the point $\Delta_0 = 0$.

In Fig. 2(a), it is shown that for a short pulse with a duration $\tau = 1$ ps, an increase in the inhomogeneous linewidth from $\gamma_2^* = 0.005$ to $\gamma_2^* = 0.1$ reduces the antisymmetric contribution $\mathrm{Re}\varepsilon_{\mathrm{res}}(x, \omega)$ (lines 3 and 4) to the resonant permittivity by almost an order of magnitude in the region of the spectral width of the pulse (dotted line 5). At the edges of the function $g(\Delta - \Delta_0) = g(\omega_0 - \omega_0')$ (line 6), the value $\mathrm{Re}\varepsilon_{\mathrm{res}}(x, \omega)$ increases significantly, but this occurs outside the pulse spectrum. The ratio $|\Delta_{PT}(x, \omega)/\mathrm{Im}\varepsilon_{\mathrm{res}}(x, \omega)|$ in the region of the pulse spectrum also decreases significantly with increase of γ_2^* [Fig. 2(b)].

It is clearly seen from Eq. (4) that quasi-$\mathcal{PT}$-symmetry can also be realized by increasing the width of a homogeneously broadened line $\sim 1/T_2$. However, it is apparently much easier to achieve a significant increase in the inhomogeneous broadening of the spectral line, for example, using well-known optics glass doped with resonant ions [27] or structures with quantum dots [28]. In solid-state structures, a large homogeneous broadening is observed much less frequently; Ti-sapphire crystals [29] are more likely an exception.

The quasi-$\mathcal{PT}$-symmetry allows one to consider the dynamics of broadband short spatially localized pulses in a medium with material dispersion, as well as to investigate specific quasi-$\mathcal{PT}$-symmetric dynamic effects for a pulse. In the next section, we consider the boundary problem of dynamical Bragg diffraction in the Laue geometry of picosecond pulse in a quasi-$\mathcal{PT}$-symmetric PhC with strong dispersion.

III. DYNAMICAL BRAGG DIFFRACTION OF SHORT PULSE IN QUASI-$\mathcal{PT}$-SYMMETRIC PHOTONIC CRYSTALS UNDER THE LAUE SCHEME

Let an s-polarized short optical pulse

$$E_{in}(\mathbf{r}, t) = A_{in}(\mathbf{r}, t) \exp(i\mathbf{k}_0 \cdot \mathbf{r} - i\omega_0 t) \tag{7}$$

with slowly varying amplitude $A_{in}(\mathbf{r}, t)$ and a finite spectral width $\delta\omega$ be incident at an angle θ onto the surface $z = 0$ of one-dimensional dispersive quasi-$\mathcal{PT}$-symmetric PhC (Fig. 1) with dielectric permittivity (1). Here, $\mathbf{k}_0 = (k_{0x}, k_{0z})$ is the central wave vector in a vacuum, $k_0 = \omega_0/c = 2\pi/\lambda_0$, ω_0 is the central frequency of the pulse, c is the speed of light in a vacuum, λ_0 is the wavelength, $k_{0x} = k_0 \sin\theta$, and $k_{0z} = k_0 \cos\theta$. The pulse duration τ is assumed to be rather long, i.e., $\tau \gg T_2$, T_2^*, so that it is possible to ensure the quasi-$\mathcal{PT}$-symmetry of the structure-pulse interaction in the presence of material dispersion.

The real field in the PhC, $\tilde{E}(\mathbf{r}, t)$, obeys the wave equation

$$\Delta\tilde{E}(\mathbf{r}, t) - \frac{1}{c^2}\frac{\partial^2\tilde{D}(\mathbf{r}, t)}{\partial t^2} = 0, \tag{8}$$

where $\Delta = \partial^2/\partial x^2 + \partial^2/\partial z^2$ is the Laplacian, and $\tilde{D}(\mathbf{r}, t) = \tilde{E}(\mathbf{r}, t) + 4\pi\tilde{P}(\mathbf{r}, t)$ is the electric field induction. For a linear isotropic medium, whose properties do not change with time, in accordance with the principle of causality, polarization $\tilde{P}(\mathbf{r}, t)$ can be represented as a material integral relation,

$$\tilde{P}(\mathbf{r}, t) = \int_0^\infty \tilde{\chi}(x, \tau')\tilde{E}(\mathbf{r}, t - \tau')d\tau', \tag{9}$$

where $\tilde{\chi}(x, \tau')$ is the real function that takes into account the dependence of polarization on the fields acting at previous points in time $t - \tau'$, and τ' is the delay time. Represent the field $\tilde{E}(\mathbf{r}, t)$ in Eqs. (8) and (9) as a Fourier integral,

$$\tilde{E}(\mathbf{r}, t) = \int_{-\infty}^\infty \tilde{E}(\mathbf{r}, \omega)\exp(-i\omega t)d\omega. \tag{10}$$

Substitution of Eq. (10) into Eqs. (8) and (9) and subsequent transition to the complex field $E(\mathbf{r}, t)$, i.e., $\tilde{E}(\mathbf{r}, t) = (1/2)[E(\mathbf{r}, t) + \mathrm{c.c.}]$, leads to the wave equation in the spectral representation for the complex field:

$$\Delta E(\mathbf{r}, \omega) + k^2\varepsilon(x, \omega)E(\mathbf{r}, \omega) = 0, \tag{11}$$

where $E(\mathbf{r}, \omega) = (1/2\pi)\int_{-\infty}^{\infty} E(\mathbf{r}, t)\exp(i\omega t)dt$, $k = \omega/c$, $\varepsilon(x, \omega) = 1 + 4\pi\chi(x, \omega)$ is the complex dielectric permittivity, and

$$\chi(x, \omega) = \int_0^\infty \tilde{\chi}(x, \tau')\exp(i\omega\tau')d\tau'. \tag{12}$$

We expand the periodic function $\varepsilon(x, \omega)$ in series by the reciprocal lattice vectors

$$\varepsilon(x, \omega) = \sum_{m=-\infty}^{\infty} \varepsilon_m(\omega)\exp(-imhx), \tag{13}$$

where

$$\varepsilon_m(\omega) = (1/d)\int_0^d \varepsilon(x, \omega)\exp(imhx)dx. \tag{14}$$

To solve the problem of pulse propagation in a periodic medium with a function of the dielectric permittivity (1), we use the spectral method [30,31]. The field of the incident pulse (7) on the surface $z = 0$ is expressed in the form of a two-dimensional Fourier integral,

$$E_{in}(x, t) = \int_{-\infty}^{+\infty}\int_{-\infty}^{+\infty} E_{in}(k_x, \omega)\exp(ik_x x - i\omega t)dk_x d\omega, \tag{15}$$

where

$$E_{in}(k_x,\omega)\equiv A_{in}(K,\Omega)=\frac{1}{(2\pi)^2}\int_{-\infty}^{+\infty}\int_{-\infty}^{+\infty}A_{in}(x,t)\times\exp(-iKx+i\Omega t)dxdt, \tag{16}$$

and $\Omega=\omega-\omega_0$, $K=k_x-k_{0x}$. Next, we solve the Bragg diffraction problem for a single spectral component, i.e., a plane monochromatic wave, and carry out Fourier synthesis to find the pulse field $E(\mathbf{r},t)$ at each point of the medium at any time instant.

Near the Bragg condition $2k_0\sin\theta_B=sh$, where θ_B is the Bragg angle, the field into the periodic structure can be represented in a two-wave approximation as a sum of two strongly coupled transmitted, E_0, and diffracted, E_h, waves,

$$E(\mathbf{r},\omega)=E_0(\mathbf{r},\omega)+E_h(\mathbf{r},\omega), \tag{17}$$

where, taking into account relation (13),

$$E_g(x,z,\omega)=\int_{-\infty}^{\infty}A_g(K,\Omega)\exp[i(q_{0x}-sg)x+iq_{0z}z]dK. \tag{18}$$

Here, $g=0,\ h;\ s=1$ if $\theta>0$ and $s=-1$ if $\theta<0$ (Fig. 1), and $A_0(K,\Omega)$ and $A_h(K,\Omega)$ are amplitudes of the spectral components of transmitted and diffracted waves, respectively. Due to the conservation of the tangential components of the wave vectors on the boundary $z=0$, the x projection of the wave vectors of the transmitted waves within the medium is $q_{0x}(K)=k_x=k_{0x}+K$. Explicit view of the z projections $q_{0z}=q_{hz}$ is presented below [Eq. (21)]. The full field $E(x,z,t)$ is obtained by substituting Eqs. (17) and (18) into the Fourier integral,

$$E(x,z,t)=\int_{-\infty}^{\infty}[E_0(x,z,\omega)+E_h(x,z,\omega)]\exp(-i\omega t)d\omega. \tag{19}$$

Substitution of Eqs. (13), (17), and (18) into the wave equation (11) results in the following system of equations for the amplitudes of the fields $A_{0,h}(K,\Omega)$:

$$\left(\varepsilon_0k^2-q_{0x}^2-q_{0z}^2\right)A_0+\varepsilon_{-s}k^2A_h=0, \tag{20a}$$

$$\varepsilon_sk^2A_0+\left[\varepsilon_0k^2-(q_{0x}-sh)^2-q_{0z}^2\right]A_h=0, \tag{20b}$$

where $\varepsilon_1=[\varepsilon'-\hat{\varepsilon}(\omega)]/2$, $\varepsilon_{-1}=[\varepsilon'+\hat{\varepsilon}(\omega)]/2$, and the quantities ε', $\hat{\varepsilon}(\omega)$ are introduced in Eq. (1).

The condition for the existence of nontrivial solutions of the system of Eqs. (20) allows us to write dispersion relations for z projections of wave vectors of the transmitted and diffracted waves of two eigenmodes, called the Borrmann, $q_{0z}^{(1)}$, and anti-Borrmann, $q_{0z}^{(2)}$, modes:

$$\left(q_{0z}^{(1,2)}\right)^2=k^2\left[\gamma_0^2+\alpha_s\mp\left(\alpha_s^2+\varepsilon_s\varepsilon_{-s}\right)^{1/2}\right], \tag{21}$$

where $\gamma_0=\sqrt{\varepsilon_0-(q_{0x}/k)^2}$, and

$$\alpha_s=(sq_{0x}-h/2)h/k^2 \tag{22}$$

defines the degree of detuning from the exact Bragg condition $q_{0x}=sh/2$. For radiation with a frequency $\omega=\omega_0$, it follows from Eq. (22) that in the vicinity of the Bragg condition, a simpler relation is satisfied: $\alpha_s=\Delta\theta\sin(2|\theta_B|)$, where $\Delta\theta=\theta-\theta_B\ll\theta_B$. Dispersion relations for the diffracted waves are obtained by the replacement $q_{0x}=q_{hx}+sh$ and $q_{0z}^{(1,2)}=q_{hz}^{(1,2)}$ into Eq. (21). From Eq. (20a), we obtain the relations connecting the amplitudes of direct and diffracted waves,

$$A_{hj}=R_jA_{0j},\quad R_{1,2}=\left[\alpha_s\mp\left(\alpha_s^2+\varepsilon_s\varepsilon_{-s}\right)^{1/2}\right]/\varepsilon_{-s}, \tag{23}$$

where R_j are partial amplitude coefficients of diffraction reflection of the waves; and A_{0j} and A_{hj} are amplitudes of the Borrmann ($j=1$) and anti-Borrmann ($j=2$) modes.

Considering a specular reflection from the input boundary of the PhC, the expressions for the amplitudes of the fields in one-dimensional PhC are found from the continuity conditions for the tangential components of the electric and magnetic fields at the boundary $z=0$:

$$\begin{aligned}A_{in}+A_S&=A_{01}+A_{02},\\ k_z(A_{in}-A_S)&=q_{0z}^{(1)}A_{01}+q_{0z}^{(2)}A_{02},\\ R_1A_{01}+R_2A_{02}&=0,\end{aligned} \tag{24}$$

where A_S is the amplitude of the specularly reflected wave. The solution of the system (24) is

$$A_{01}=-[(1+R_S)R_2/R_{12}]A_{in},\quad A_{02}=[(1+R_S)R_1/R_{12}]A_{in}, \tag{25}$$

where $R_{12}=R_1-R_2$, $R_S=A_S/A_{in}=(k_z-f_S)/(k_z+f_S)$ is the diffraction-modified Fresnel reflection coefficient, $f_S=(q_{0z}^{(2)}R_1-q_{0z}^{(1)}R_2)/R_{12}$, and $k_z=\sqrt{k^2-k_x^2}$.

The total field, Eqs. (19) and (25), of the pulse at each point of the PhC at any time is given by the following expression:

$$E(\mathbf{r},t)=[A_0(\mathbf{r},t)+A_h(\mathbf{r},t)\exp(-ishx)]\exp(ik_{0x}x-i\omega_0t), \tag{26}$$

where

$$A_g(\mathbf{r},t)=\int_{-\infty}^{\infty}\int_{-\infty}^{\infty}\left(A_{g1}e^{iq_{0z}^{(1)}z}+A_{g2}e^{iq_{0z}^{(2)}z}\right)e^{iKx-i\Omega t}dKd\Omega,\quad(g=0,\ h), \tag{27}$$

and the amplitudes A_{gj} are determined from the relations (23) and (25).

For greater clarity of the effects under study, we consider in detail analytically the case of weak specular reflection of radiation from the boundary $z=0$, $A_S\ll A_{in}$, using the corresponding values of the PhC parameters. So, let the amplitude of the incident field be $A_{in}=1$; then, from the boundary conditions in the case of neglect of reflection, it follows that $A_{01}+A_{02}=1$ and $A_{h1}+A_{h2}=0$. Using the expressions (23), we get

$$A_{01}=-\frac{R_2}{R_1-R_2},\quad A_{02}=\frac{R_1}{R_1-R_2}, \tag{28}$$

where

$$\frac{R_{1,2}}{R_1-R_2}=\frac{-\alpha_s\pm\left(\alpha_s^2+\varepsilon_s\varepsilon_{-s}\right)^{1/2}}{2\left(\alpha_s^2+\varepsilon_s\varepsilon_{-s}\right)^{1/2}}. \tag{29}$$

Let us obtain the amplitudes of the fields at different signs of the angles of incidence $\theta>0$ and $\theta<0$, i.e., $s=1$ and $s=-1$, respectively, in cases of different values of gain and loss parameter of the medium $\hat{\varepsilon}(\omega)$. The first one is $\hat{\varepsilon}(\omega)=\varepsilon'$,

and as a result $\varepsilon_1 = [\varepsilon' - \hat{\varepsilon}(\omega)]/2 = 0$. This is an exceptional point (EP) of the $\mathcal{PT}$-symmetry breaking. The second case is below the EP threshold $\hat{\varepsilon}_R(\omega) < \varepsilon'$ when there exists the propagation of orthogonal Borrmann and anti-Borrmann modes [Eq. (21)]. The degree of proximity to the EP will be characterized by the parameter $\eta = \hat{\varepsilon}_R(\omega_0)/\varepsilon'$.

As it follows from Eqs. (28) and (29), in the EP, the amplitudes of transmitted waves $A_{01,02}$ do not depend on the sign of the angle θ, but depend on the sign of the detuning α_s on the exact Bragg angle. Indeed, with $\varepsilon_s = 0$ and $\alpha_s > 0$ values,

$$R_{1,2}/(R_1 - R_2) = (-\alpha_s \pm |\alpha_s|)/2|\alpha_s| = 0;\ -1.$$

Then,

$$A_{01} = 1, \quad A_{02} = 0. \tag{30}$$

If $\alpha_s < 0$, then

$$A_{01} = 0, \quad A_{02} = 1 \tag{31}$$

[Fig. 3(a)]. Under the exact Bragg condition $\alpha_s = 0$, as can be seen from Eqs. (28) and (29), in the EP: $A_{01} = A_{02} = 1/2$.

In contrast to the amplitudes of the transmitted waves, the amplitudes of the diffracted waves $A_{h1,h2}$ in the EP and around it depend radically on the sign of the angle of incidence θ and do not depend on the sign of the detuning α_s. Let us show it. From Eqs. (23), (28), and (29), it is easy to obtain that

$$A_{h2} = \frac{\varepsilon_s}{2\left(\alpha_s^2 + \varepsilon_s\varepsilon_{-s}\right)^{1/2}}. \tag{32}$$

From this expression, it follows that when $\theta > 0$ at EP, the magnitude $\varepsilon_s = \varepsilon_1 \equiv (\varepsilon' - \hat{\varepsilon})/2 = 0$ and amplitudes $A_{h1} = -A_{h2} = 0$, i.e., diffracted waves are missing [curves 1 and 2 in Fig. 3(b)]. If the angle $\theta < 0$, then $\varepsilon_s = \varepsilon_{-1} \equiv (\varepsilon' + \hat{\varepsilon})/2 \neq 0$, $\varepsilon_{-s} = \varepsilon_1 = 0$, and the amplitudes $A_{h2} = -A_{h1} = \varepsilon_{-1}/2|\alpha_s|$ tend to infinity if $\alpha_s \to 0$ [curves 3 and 4 in Fig. 3(b)]. In this case, the field of diffracted waves, given by Eq. (33), in the PhC of finite thickness is the final value and increases linearly in z [inset in Fig. 3(b)]. Indeed, in the case of exact Bragg condition $\alpha_{-1} = 0$, the full field of diffracted plane waves,

$$\begin{aligned} E_h(x, z; \omega, q_{0x}) &= E_{h1}(x, z; \omega, q_{0x}) + E_{h2}(x, z; \omega, q_{0x}) \\ &= A_{h1}\left[\exp\left(iq_{0z}^{(1)}z\right) - \exp\left(iq_{0z}^{(2)}z\right)\right] \\ &\quad \times \exp[i(q_{0x} - sh)x], \end{aligned} \tag{33}$$

at small $\varepsilon_1\varepsilon_{-1} \ll \gamma_0$ and $|\alpha_s| \ll \gamma_0$, is determined by the expression

$$E_h(x, z; \omega, q_{0x}) \approx i(\varepsilon_{-1}kz/2\gamma_0)\exp[i(q_{0x} - sh)x + ik\gamma_0 z]. \tag{34}$$

Thus, despite a significant increase in the amplitudes of the diffracted waves $A_{hj} \to \mp\infty$ near the EP, the simultaneous fulfillment of the condition $q_{0z}^{(1,2)} \to k\gamma_0$ [Eq. (21)] leads to a linear increase of the amplitude of the total field E_h (34) within the PhC with depth $z \ll \lambda_0\gamma_0/\pi\sqrt{\alpha_s^2 + \varepsilon_1\varepsilon_{-1}}$.

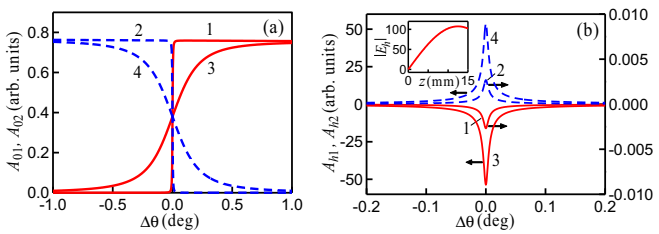

FIG. 3. (a) Dependences of amplitudes A_{01} (curves 1 and 3) and A_{02} (curves 2 and 4) on the detuning $\Delta\theta = \theta - \theta_B$ from the exact Bragg angle near EP when $\eta = 0.9999$ (curves 1 and 2) and far from EP when $\eta = 0.5$ (curves 3 and 4); they do not depend on the sign of the angle θ. (b) Dependences of amplitudes A_{h1} (curves 1 and 3) and A_{h2} (curves 2 and 4) on $\Delta\theta$ near EP ($\eta = 0.9999$) when $\theta > 0$ (curves 1 and 2) and $\theta < 0$ (curves 3 and 4). Inset: the dependence of the full field of diffracted waves $|E_h|$ on the depth z near the ET at $\theta < 0$. Parameters: $\lambda = 1\ \mu$m, $d = 1\ \mu$m, $\varepsilon_0 = 2.25$, $\varepsilon' = 0.008$. All curves are given taking into account specular reflection from the entrance surface of the PhC [Eqs. (23)–(25)].

IV. PULSE PROPAGATION AND UNIDIRECTIONAL BRAGG-DIFFRACTION-INDUCED PULSE SPLITTING IN QUASI-$\mathcal{PT}$-SYMMETRIC PHOTONIC CRYSTAL

As shown above, the amplitudes of the spectral components of transmitted and diffracted waves in a quasi-$\mathcal{PT}$-symmetric PhC near an EP significantly depend on the sign of the angle of incidence θ and the deviation α_s from the exact Bragg condition. Therefore, we can rightly expect that the dynamics of optical pulses near an EP in a quasi-$\mathcal{PT}$-symmetric PhC will have a number of features uncharacteristic for a conservative PhC.

Let the Gaussian spatially confined pulse (7) with amplitude

$$A_{in}(x, 0, t) = A\exp[-(x\cos\theta/r_0)^2 - (t - x\sin\theta/c)^2/\tau^2] \tag{35}$$

be incident at the angle θ onto the surface $z = 0$ of PhC. Here, r_0 is the transverse size of the pulse and τ is the pulse duration.

We select the structure and radiation parameters in such a way that the EP condition $\hat{\varepsilon}(\omega_0) = \varepsilon'$ and the Bragg condition $\alpha_s = 0$ for the center frequency of the pulse are exactly fulfilled. In Fig. 4, using solutions (26) and (27), we show the spatial distribution of the intensity of the pulse field, $|E(x, z, t)|^2$, at different times, with $\theta > 0$ (upper panels) and $\theta < 0$ (lower panels). We also consider the different pulse durations, as well as the cases of dispersive breaking of $\mathcal{PT}$ symmetry and the existence of quasi-$\mathcal{PT}$-symmetry. In Figs. 4(a) and 4(b), the intensity of the field of an extended quasimonochromatic pulse with long duration $\tau = 100$ ps and the longitudinal size $\tau c \gg L$, where L is the thickness of the PhC, is represented. If $\theta > 0$, the pulse propagates in a periodic Bragg structure with absorption and amplification as in a continuous conservative medium, i.e., without diffraction [in accordance with Eqs. (23), (30), and (31), $E_h = 0$ at $\varepsilon_1 = 0$] and without gain or loss. The medium is transparent. With the sign of angle changing $\theta < 0$ [Fig. 4(b)], the pulse Bragg diffraction occurs, as well as its significant amplification and spatial expansion, similar to the gain saturation described earlier for monochromatic beams [18]. The output pulse in the forward direction is not amplified, while the diffracted pulse is amplified many times. The dynamics of an extended

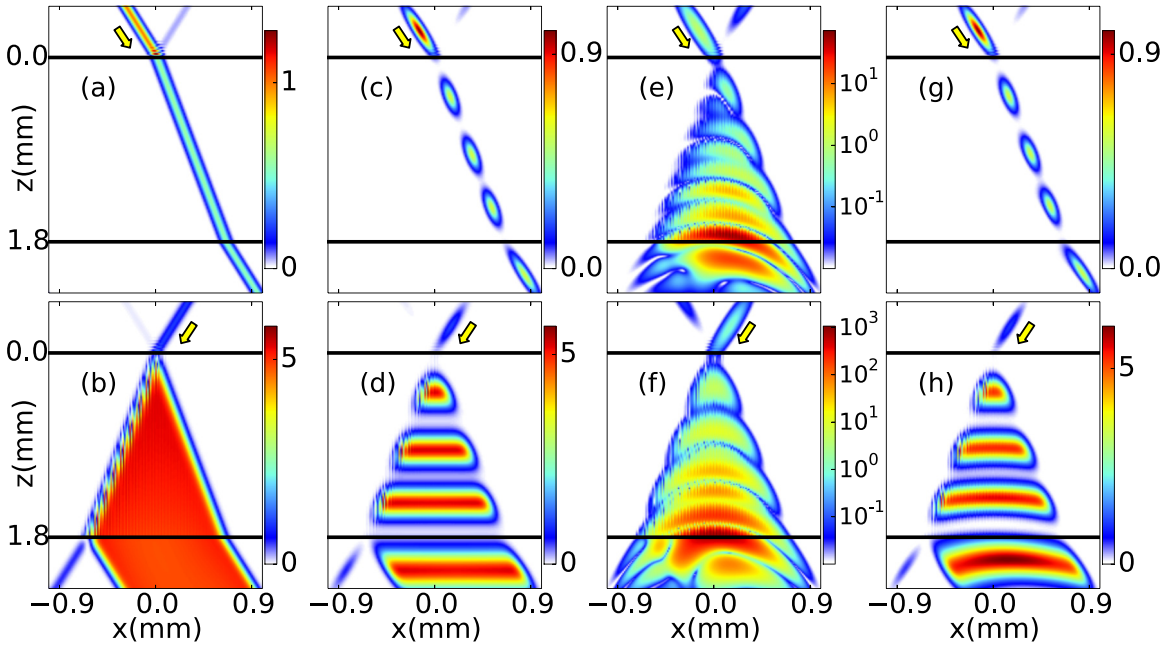

FIG. 4. The intensity of the pulse field $|E(x,z,t)|^2$ at different points in time in EP at the angles of incidence $\theta = \theta_B = +30^0$ (upper panels) and $\theta = \theta_B = -30^0$ (lower panels). (a), (b) Gaussian pulse duration $\tau = 100$ ps; (c)–(h) $\tau = 1$ ps. Parameters: inhomogeneous broadening (e), (f) $\gamma_2^* = 0.005$ and (g), (h) $\gamma_2^* = 0.1$; the magnitude of the homogeneous broadening $\gamma_2 = 0.005$, $\lambda_0 = 1$ μm, $d = 1$ μm, $\varepsilon_0 = 2.25$, $\varepsilon' = 0.008$, $\eta(\omega_0) = 0.9999$, the transverse radius of the pulse $r_0 = 60$ μm, the times in the panels: (a), (b) $t = 1$ ps and (c)–(h) $t = -1,\ 2,\ 5,\ 8,\ 11$ ps. The black lines indicate the crystal boundaries $z = 0$ and $z = L = 1.8$ mm; the arrows indicate the directions of pulse falling on the PhC.

quasimonochromatic pulse in a thin PhC with dispersion is almost the same as the dynamics of a monochromatic beam, and the effect of unidirectional diffraction Bragg reflection is observed.

Figures 4(c) and 4(d) represent the dynamics of a short pulse with $\tau = 1$ ps in different moments of time, but in the case when, formally mathematically, the frequency dependence is not taken into consideration in the dielectric permittivity, $\hat{\varepsilon}(\omega) = \text{const}$ in Eq. (1), i.e., the disruptive effect of dispersion on $\mathcal{PT}$ symmetry is not formally taken into account. The only difference of these snapshots from Figs. 4(a) and 4(b) is in the possibility to observe the localization of the pulse in the medium at different points in time due to the short pulse duration.

Accounting for physically real material dispersion with a small inhomogeneous broadening, $\gamma_2^* = 0.005$, leads to a breaking of $\mathcal{PT}$ symmetry for a broadband short pulse with a duration $\tau = 1$ ps and, as a consequence, to the disappearance of the $\mathcal{PT}$-symmetric effect of unidirectional Bragg diffraction reflection with a change in the sign of the angle of incidence [Figs. 4(e) and 4(f)]. The intensity distributions in Figs. 4(e) and 4(f) are not fundamentally different. It is important to note that in the case of a thick PhC with a thickness $L \gg \tau c$, the quasimonochromatic pulse, $\tau = 100$ ps, localized in the structure also begins to decay despite the small width of the pulse spectrum. The dynamics of the pulse in this case will have the characteristic features similar to Figs. 4(e) and 4(f), which qualitatively differs from Figs. 4(a) and 4(b) for a thin PhC with $L \ll \tau c$. Numerical calculations show that the characteristic depth of the PhC L_c, at which the pulse dynamics loses its $\mathcal{PT}$-symmetric properties and the pulse is destroyed, can be estimated as follows: $L_c \approx 1/|\text{Im}[q_{0z}^{(1,2)}(\Delta\Omega_c)]|$, where $\Delta\Omega_c = 1/\tau$.

Finally, we create a quasi-$\mathcal{PT}$-symmetry condition, increasing the magnitude of the inhomogeneous broadening by an order of magnitude $\gamma_2^* = 0.1$, while retaining all the other parameters. This leads to dramatic changes in the dynamics of the pulse [Figs. 4(g) and 4(h)]. The $\mathcal{PT}$-symmetric properties of the medium are almost completely restored, and unidirectional diffraction reflection is observed for a short localized pulse with a change in the sign of the Bragg angle. At a positive angle of incidence, a short pulse propagates in a quasi-$\mathcal{PT}$-symmetric PhC as in a transparent homogeneous medium—without diffraction reflection and change of parameters [Fig. 4(g)]. A change in the sign $\theta < 0$ results in the appearance of an amplified diffracted pulse [Fig. 4(h)]. Moreover, the snapshots of the intensity in Figs. 4(g) and 4(h) for a realistic physical model of a medium with a material dispersion are close to the idealized formally mathematical case of $\mathcal{PT}$ symmetry without taking into account dispersion [compare with Figs. 4(c) and 4(d)]. In Figs. 4(g) and 4(h), it is also clearly seen that the quasi-$\mathcal{PT}$-symmetric dynamics of a short pulse persists at the depth of propagation in the PhC for more than ten pulse lengths, whereas without quasi-$\mathcal{PT}$-symmetry, the localized pulse already decays at a depth of the order of several pulse lengths. In addition, the dynamics of a pulse in a quasi-$\mathcal{PT}$-symmetric PhC in Figs. 4(g) and 4(h), under Bragg condition and at EP, is radically different from the pulse dynamics in a conservative PhC. In the latter case, a temporal splitting of the pulse is observed due to the orthogonality of the Borrmann and anti-Borrmann modes [30–32], whereas in quasi-$\mathcal{PT}$-symmetric PhC at EP, these

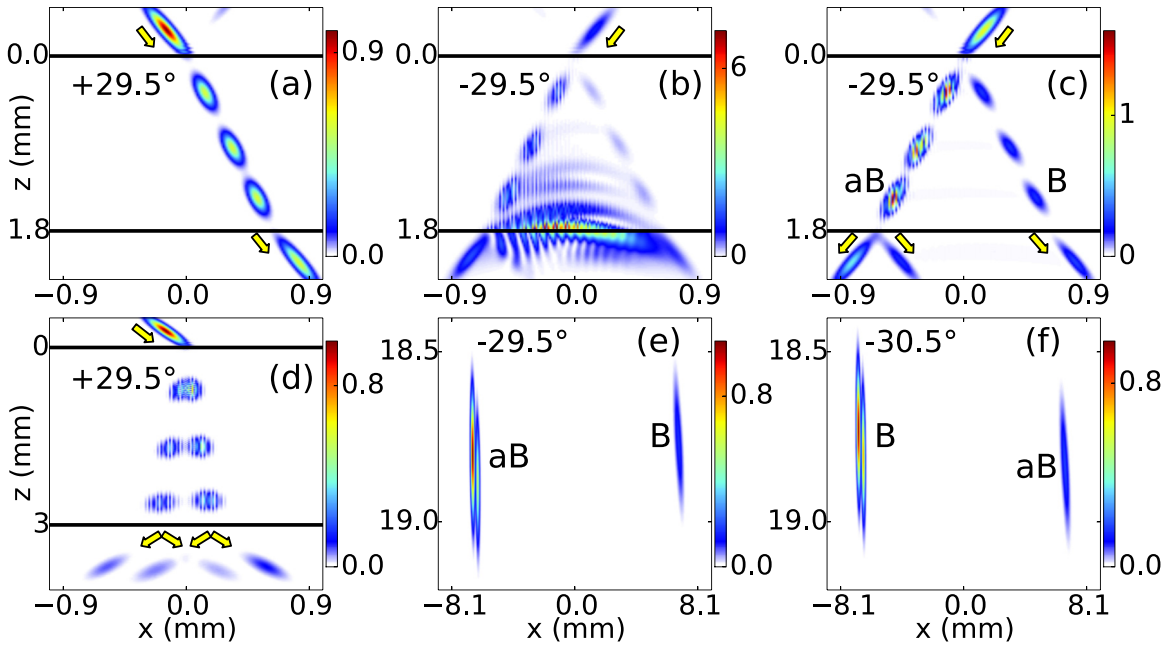

FIG. 5. (a)–(c), (e), (f) The intensity of the pulse field $|E(x, z, t)|^2$ in the EP and under small deviation $\alpha_s \neq 0$ from exact Bragg condition at different points in time t. (a)–(e) $\alpha_s < 0$; (a) angle of incidence $\theta = +29.5^0$(shown in panels), $\gamma_2^* = 0.1$; (b) $\theta = -29.5^0$, $\gamma_2^* = 0.005$; (c) $\theta = -29.5^0$, $\gamma_2^* = 0.1$; $t = -1,\ 2,\ 5,\ 8,\ 11$ ps. (e) $\theta = -29.5^0$, $t = 100$ ps; (f) $\alpha_s > 0$, $\theta = -30.5^0$, $t = 100$ ps. (a)–(d) $r_0 = 60$ μm; (e), (f) $r_0 = 300$ μm; (a)–(c), (e), (f) $\varepsilon' = 0.008$, $\eta = 0.9999$; (d) $\varepsilon' = 0.08$, $\varepsilon_{\text{res}} = 0$, $t = -1,\ 3,\ 7,\ 11,\ 15$ ps. Other parameters are as in Fig. 4. Letters "B" and "aB" indicate Borrmann and anti-Borrmann pulses.

modes are nonorthogonal [from Eq. (21), it follows that $q_{0z}^{(1)} = q_{0z}^{(2)} = k\gamma_0$] and there is no temporal pulse splitting.

With the choosing of a small deviation $\alpha_s \neq 0$ from the exact Bragg condition at EP with $\theta > 0$, the pulse propagation dynamics [Fig. 5(a)] is similar to the case $\alpha_s = 0$ discussed above [Fig. 4(g)] and practically does not depend on the sign of the detuning α_s. A small change α_s in the angle of incidence leads only to a change in the angle of refraction of the pulse in the structure, as in a homogeneous transparent medium. The amplitudes of the diffracted waves remain negligibly small.

With the changing in sign $\theta < 0$ at $\alpha_s \neq 0$, the pulse dynamics becomes much more complicated—spatial diffraction splitting of the pulse occurs [Figs. 5(b) and 5(c)]. However, as can be seen from Fig. 5(b), in a dispersive PhC with a small inhomogeneous line broadening $\gamma_2^* = 0.005$, the separated pulses already quickly lose localization at a small depth on the order of several pulse sizes. At a quasi-$\mathcal{PT}$-symmetry, i.e., at increasing in broadening up to $\gamma_2^* = 0.1$, the pulse reveals spatial and temporal diffraction-induced splitting into the Borrmann (B) and anti-Borrmann (aB) pulses [Fig. 5(c)], which are formed by the Borrmann and anti-Borrmann modes, respectively. Here the unidirectional diffraction-induced splitting is observed, in contrast to the case of a conservative PhC [Fig. 5(d)], when the pulse splitting does not depend on the sign of the incident angle [30–32]. In addition, there are differences in the amplitudes and the structure of the separated pulses compared with the conservative PhC. The amplitudes of the pulses are amplified by increasing the amplitudes of the diffracted waves, A_{h1} and A_{h2}, given by Eq. (32). The direct wave exists only in the Borrmann pulse if $\alpha_s > 0$ and in the anti-Borrmann pulse if $\alpha_s < 0$, in accordance with Eq. (30) and Eq. (31). In Fig. 5(c), it is seen that at the output of PhC, the transmitted anti-Borrmann pulse disintegrates into direct and amplified diffracted pulses, while the outgoing Borrmann pulse propagates in the direction of the diffracted wave since it is formed inside the PhC only by the diffracted wave. Within the PhC in Fig. 5(c), the intensity oscillations of the anti-Borrmann pulse occur because of the superposition of transmitted and diffracted waves. The intensity of the Borrmann pulse does not oscillate, and the pulse consists of only a diffracted field.

When the sign of detuning from the exact Bragg condition α_s changes, the Borrmann and anti-Borrmann impulses change places [Figs. 5(e) and 5(f)]. The interference of direct and diffracted waves leads to oscillations, clearly visible on the left pulses in Figs. 5(e) and 5(f). There are no oscillations in the right pulses since there are no direct waves in them ($A_{01} = A_{02} = 0$). From Figs. 5(e) and 5(f), it is also seen that the group velocity of the Borrmann pulse is less than that of the anti-Borrmann pulse, $V_z^{(1)} < V_z^{(2)}$. Below it will be shown that this is typical for $\mathcal{PT}$-symmetric PhCs at EP [see Fig. 6(a)]. In the case of detuning from EP, as well as in a conservative PhC, the Borrmann pulse is always ahead of the anti-Borrmann pulse in a fairly wide range of angles near the Bragg condition [Fig. 6(b)].

To explain this unusual pulse dynamics, we obtain the expressions for the z and x projections of their group velocities $V_z^{(1,2)}$ and $V_x^{(1,2)}$, respectively. We take into account that in the case of broadband quasi-$\mathcal{PT}$-symmetry, the material dispersion in the region of the pulse spectrum is small compared to grating-induced dispersion, and therefore, it slightly affects the magnitude of the group velocity. So, in calculating the

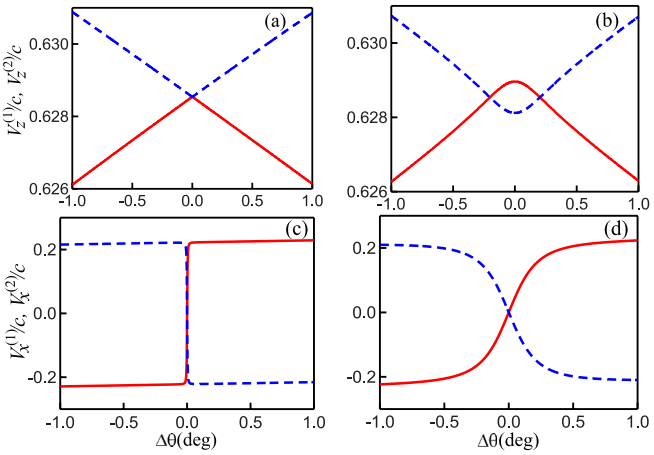

FIG. 6. (a) Group velocities $V_z^{(1)}$ (solid lines) and $V_z^{(2)}$ (dashed lines) vs angular detuning $\Delta\theta$ near the EP, $\eta = 0.9999$, and (b) far from the ET, $\eta = 0.5$. Velocities $V_z^{(1,2)}$ do not depend on the sign of the angle of incidence θ. (c) The transverse group velocities $V_x^{(1)}$ (solid lines) and $V_x^{(2)}$ (dashed lines) vs $\Delta\theta$ near the EP, $\eta = 0.9999$, and (d) far from the ET, $\eta = 0.5$, when $\theta > 0$. Other parameters are the same as those in Fig. 3.

group velocities, we consider only the grating-induced dispersion. From the dispersion relation (21), for group velocities $V_z^{(1,2)} = (\partial\omega/\partial q_{0z}^{(1,2)})|_{q_{0x}=\text{const}}$, we obtain

$$V_z^{(1,2)} = \frac{c q_{0z}^{(1,2)} W}{k(\varepsilon_0 W \mp \varepsilon_1\varepsilon_{-1})}, \tag{36}$$

where $W = (\alpha_s^2 + \varepsilon_1\varepsilon_{-1})^{1/2}$. Exactly at the EP, the value $\varepsilon_1 = 0$; then,

$$V_z^{(1,2)} = (c/\varepsilon_0)(\varepsilon_0 - \sin^2\theta + \alpha_s \mp |\alpha_s|)^{1/2}. \tag{37}$$

The dependences of these velocities on the angular detuning $\Delta\theta = \theta - \theta_B$ at the central frequency of the pulse are shown in Fig. 6. From Fig. 6(a), it is seen that when the Bragg condition $\alpha_s = 0$ is fulfilled exactly, the group velocities (37) coincide and are equal to the velocity in a homogeneous medium with a dielectric constant ε_0:

$$V_z^{(1,2)} = (c/\varepsilon_0)(\varepsilon_0 - \sin^2\theta)^{1/2}. \tag{38}$$

In this case, the diffraction splitting of pulses does not occur, which corresponds to the dynamics of the pulse in Figs. 4(g) and 4(h).

With a nonzero detuning $\alpha_s \neq 0$, the Borrmann pulse always lags behind, $V_z^{(1)} < V_z^{(2)}$, independently of the signs of the angle θ and of the detuning α_s [Fig. 6(a); Figs. 5(e) and 5(f)]. Inequality of group velocities, $V_z^{(1)} \neq V_z^{(2)}$, leads to diffraction-induced temporal splitting of the pulses [Figs. 5(c), 5(e), and 5(f)].

Beyond the EP, the ratio between group velocities is reversed. As it follows from Fig. 6(b), independently of the angle θ sign, in a certain interval of angular detuning, the inequality $V_z^{(1)} > V_z^{(2)}$ takes place. Therefore, the Borrmann pulse is ahead of the anti-Borrmann one.

The transverse components of the group velocities $V_x^{(1,2)} = (\partial\omega/\partial q_{0x}^{(1,2)})|_{q_{0z}=\text{const}}$ are given by the following expressions:

$$V_x^{(1,2)} = \frac{s\alpha_s ck(W \pm h^2/2k^2)}{h(\varepsilon_0 W \mp \varepsilon_1\varepsilon_{-1})}. \tag{39}$$

Exactly at the EP and near the Bragg condition, when $|\alpha_s| \ll h^2/2k^2$, we obtain

$$V_x^{(1,2)} = \frac{s\alpha_s ck}{h\varepsilon_0}\left(1 \pm \frac{h^2}{2k^2|\alpha_s|}\right) \approx \pm\frac{s\alpha_s ch}{2|\alpha_s|k\varepsilon_0}. \tag{40}$$

As it follows from Eq. (40), the signs of the velocities $V_x^{(1,2)}$ depend on the sign of the angle of incidence, which is determined by the parameter s as well as on the sign of the detuning α_s. When $s = +1$ ($\theta > 0$), the Borrmann pulse propagates to the right with $V_x^{(1)} > 0$, if $\alpha_s > 0$, and to the left with $V_x^{(1)} < 0$, if $\alpha_s < 0$ [Figs. 6(c) and 6(d)]. Anti-Borrmann pulses propagate in opposite directions with velocities $V_x^{(2)}$. However, in this case, both diffracted waves [Eq. (32)] are absent, and, moreover, when $\alpha_s > 0$, there is no anti-Borrmann direct mode, i.e., $A_{02} = 0$ [Fig. 3(a)]. Therefore, only one nonzero mode with the amplitude $A_{01} = 1$ propagates to the right with velocity $V_x^{(1)} > 0$. If $\alpha_s < 0$, then, on the contrary, there exists only an anti-Borrmann mode with $A_{02} = 1$, which will also have a positive velocity, $V_x^{(2)} \sim -\alpha_s > 0$. Thus, the entire wave packet of the pulse propagates to the right, as shown in Fig. 5(a). If $s = -1$ ($\theta < 0$), the signs of the velocities $V_x^{(1,2)}$ [Eq. (40)] are reversed, which corresponds to the dynamics of the pulses shown in Figs. 5(c), 5(e), and 5(f).

As can be seen from Fig. 3(a) and from the dispersion relation given by Eq. (21), under the exact Bragg condition at the EP ($\alpha_s = 0$, $\varepsilon_1 = 0$), the amplitudes and propagation constants of the direct Borrmann and anti-Borrmann waves in the PhC coincide. The group velocity of direct waves in this case is equal to $V_x = (q_{0x}/\varepsilon_0 k)c = (sh/2\varepsilon_0 k)c$, but the velocities of nonzero diffracted waves at $\theta < 0$ are directed in the opposite direction: $-V_x > 0$. This leads to a strong expansion of the pulse along the x axis at $\theta < 0$, as is clearly seen from Figs. 4(g) and 4(h).

Thus, the above analytical estimations of the velocities and amplitudes of the waves, calculated for the central spectral component of the pulse, quite well describe the propagation dynamics of the spatially localized wave packet, i.e., of the pulse as a whole, in a quasi-$\mathcal{PT}$-symmetric medium.

V. CONCLUSION

We have demonstrated the dynamics of a short spatially localized optical pulse propagating in a quasi-$\mathcal{PT}$-symmetric medium with strong material dispersion and beyond the paraxial approximation. In such a medium, the propagation of pulses with a finite frequency spectrum becomes possible due to a significant restoration of the $\mathcal{PT}$-symmetric properties of the structure under broadening of the spectral line of the resonant medium. We solved the boundary problem of short picosecond pulse propagation in quasi-$\mathcal{PT}$-symmetric PhC under the dynamic Bragg diffraction in the Laue geometry. Optical phenomena caused by the short pulse dynamics in a quasi-$\mathcal{PT}$-symmetric medium are described. Near the Bragg

condition at the EP of the spontaneous breaking of the $\mathcal{PT}$-symmetry, a unidirectional Bragg-diffraction-induced short pulse splitting is revealed. At a positive angle of incidence $\theta > 0$, the pulse propagates in a periodic quasi-$\mathcal{PT}$-symmetric structure as in a homogeneous transparent medium, i.e., without diffraction, amplification, and absorption. A change in the sign of the angle of incidence, $\theta < 0$, leads to a spatial-time splitting of the pulse, and moreover, one of the pulses being formed only by the amplified diffracted wave, and the other one by the direct and diffracted waves. In contrast to the conservative PhC, the diffraction pulse splitting does not occur at the EP when the Bragg condition is exactly fulfilled, where a significant pulse amplification appears due to enhancement of the diffracted waves. There also exists a large diffraction transverse expansion of the pulse. Numerical calculations of the pulses dynamics are in good agreement with the analytical estimations of group velocities and wave amplitudes. Thus, we have shown the possibility of the propagation of short spatially localized pulses in a quasi-$\mathcal{PT}$-symmetric medium. The described quasi-$\mathcal{PT}$-symmetric effects—asymmetry of propagation, splitting, and amplification of pulses—open wide opportunities for effective control of the parameters and dynamics of short optical pulses due to small changes in the radiation frequency, as well as the medium gain-loss parameter or the angle of radiation incidence on the structure.

ACKNOWLEDGMENTS

The authors are grateful to V. V. Konotop for useful discussions. The work was supported by the Russian Foundation for Basic Research, Grant No. 18-02-00556-a, and by the BASIS Foundation (D.T.).

[1] V. V. Konotop, J. Yang, and D. A. Zezyulin, Nonlinear waves in $\mathcal{PT}$-symmetric systems, Rev. Mod. Phys. **88**, 035002 (2016).

[2] *Parity-time Symmetry and Its Applications*, edited by D. Christodoulides and J. Yang, Springer Tracts in Modern Physics, Vol. 280 (Springer, Singapore, 2018).

[3] C. M. Bender and S. Boettcher, Real Spectra in Non-Hermitian Hamiltonians Having $\mathcal{PT}$ Symmetry, Phys. Rev. Lett. **80**, 5243 (1998).

[4] C. M. Bender, D. C. Brody, and H. F. Jones, Complex Extension of Quantum Mechanics, Phys. Rev. Lett. **89**, 270401 (2002).

[5] C. M. Bender, Making sense of non-Hermitian Hamiltonians, Rep. Prog. Phys. **70**, 947 (2007).

[6] A. Ruschhaupt, F. Delgado, and J. G. Muga, Physical realization of $\mathcal{PT}$-symmetric potential scattering in a planar slab waveguide, J. Phys. A **38**, L171 (2005).

[7] R. El-Ganainy, K. G. Makris, D. N. Christodoulides, and Z. H. Musslimani, Theory of coupled optical $\mathcal{PT}$-symmetric structures, Opt. Lett. **32**, 2632 (2007).

[8] K. G. Makris, R. El-Ganainy, D. N. Christodoulides, and Z. H. Musslimani, Beam Dynamics in $\mathcal{PT}$ Symmetric Optical Lattices, Phys. Rev. Lett **100**, 103904 (2008).

[9] C. E. Ruter, K. G. Makris, R. El-Ganainy, D. N. Christodoulides, M. Segev, and D. Kip, Observation of parity-time symmetry in optics, Nat. Phys. **6**, 192 (2010).

[10] A. Guo, G. J. Salamo, D. Duchesne, R. Morandotti, M. Volatier-Ravat, V. Aimez, G. A. Siviloglou, and D. N. Christodoulides, Observation of $\mathcal{PT}$ Symmetry Breaking in Complex Optical Potentials, Phys. Rev. Lett. **103**, 093902 (2009).

[11] S. Longhi, $\mathcal{PT}$-symmetric laser absorber, Phys. Rev. A **82**, 031801 (2010).

[12] Z. J. Wong, Y. Xu, J. Kim, K. O'Brien, Y. Wang, L. Feng, and X. Zhang, Lasing and anti-lasing in a single cavity, Nat. Photon. **10**, 796 (2016).

[13] M. Kulishov, J. M. Laniel, N. Bélanger, J. Azaña, and D. V. Plant, Nonreciprocal waveguide Bragg gratings, Opt. Express **13**, 3068 (2005).

[14] Z. Lin, H. Ramezani, T. Eichelkraut, T. Kottos, H. Cao, and D. N. Christodoulides, Unidirectional Invisibility Induced by $\mathcal{PT}$-Symmetric Periodic Structures, Phys. Rev. Lett. **106**, 213901 (2011).

[15] L. Feng, Y. Xu, W. S. Fegadolli, M. Lu, J. E. Oliveira, V. R. Almaida, Y. Chen, and A. Scherer, Experimental demonstration of a unidirectional reflectionless parity-time metamaterial at optical frequencies, Nat. Mater. **12**, 108 (2012).

[16] S. Longhi, Bloch Oscillations in Complex Crystals with $\mathcal{PT}$-Symmetry, Phys. Rev. Lett. **103**, 123601 (2009).

[17] M. V. Berry, Optical lattices with $\mathcal{PT}$ symmetry are not transparent, J. Phys. A: Math. Theor. **41**, 244007 (2008).

[18] S. Longhi, Spectral singularities and Bragg scattering in complex crystals, Phys. Rev. A **81**, 022102 (2010).

[19] V. V. Konotop and B. I. Mantsyzov, Light propagation through a $\mathcal{PT}$-symmetric photonic-crystal, Opt. Express **24**, 26146 (2016).

[20] V. A. Bushuev, L. V. Dergacheva, and B. I. Mantsyzov, Asymmetric pendulum effect and transparency change of $\mathcal{PT}$-symmetric photonic crystals under dynamical Bragg diffraction beyond the paraxial approximation, Phys. Rev. A **95**, 033843 (2017).

[21] P. A. Brandão and S. B. Cavalcanti, Bragg-induced power oscillations in $\mathcal{PT}$ -symmetric periodic photonic structures, Phys. Rev. A **96**, 053841 (2017).

[22] A. A. Zyablovsky, A. P. Vinogradov, A. V. Dorofeenko, A. A. Pukhov, and A. A. Lisyansky, Causality and phase transitions in $\mathcal{PT}$-symmetric optical systems, Phys. Rev. A **89**, 033808 (2014).

[23] A. A. Zyablovsky, A. P. Vinogradov, A. A. Pukhov, A. V. Dorofeenko, and A. A. Lisyansky, $\mathcal{PT}$ symmetry in optics, Phys. Usp. **57**, 1063 (2014).

[24] D. M. Tsvetkov, V. A. Bushuev, V. V. Konotop, and B. I. Mantsyzov, Broadband quasi-$\mathcal{PT}$-symmetry sustained by inhomogeneous broadening of the spectral line, Phys. Rev. A **98**, 053844 (2018).

[25] L. Allen and J. H. Eberly, *Optical Resonance and Two-Level Atoms* (Wiley, New York, 1975).

[26] C. Hang, G. Huang, and V. Konotop, $\mathcal{PT}$ Symmetry with a System of Three-Level Atoms, Phys. Rev. Lett. **110**, 083604 (2013).

[27] M. Ams, P. Dekker, S. Gross, and M. J. Withford, Fabricating waveguide Bragg gratings (WBGs) in bulk materials using ultrashort laser pulses, Nanophotonics **6**, 743 (2017).

[28] J. Bao and M. G. Bawendi, A colloidal quantum dot spectrometer, Nature (London) **523**, 67 (2015).

[29] W. T. Silfvast, *Laser Fundamentals* (Cambridge University, Cambridge, 2004).

[30] V. A. Bushuev, B. I. Mantsyzov, and A. A. Skorynin, Diffraction-induced laser pulse splitting in a linear photonic crystal, Phys. Rev. A **79**, 053811 (2009).

[31] A. A. Skorynin, V. A. Bushuev, and B. I. Mantsyzov, Dynamical Bragg diffraction of optical pulses in photonic crystals in the Laue geometry: Diffraction-induced splitting, selective compression, and focusing of pulses, J. Exp. Theor. Phys. **115**, 56 (2012).

[32] S. E. Svyakhovskiy, V. O. Kompanets, A. I. Maydykovskiy, T. V. Murzina, S. V. Chekalin, A. A. Skorynin, V. A. Bushuev, and B. I. Mantsyzov, Observation of diffraction-induced laser pulse splitting in a photonic crystal, Phys. Rev. A **86**, 013843 (2012).